Chemistry & Biology, Vol. 9, 1209–1217, November, 2002, ©2002 Elsevier Science Ltd. All rights reserved. PII S1074-5521(02)00245-4

Analysis of the π-π Stacking Interactions between the Aminoglycoside Antibiotic Kinase APH(3′)-IIIa and Its Nucleotide Ligands

David D. Boehr,[1] Adam R. Farley,[2] Gerard D. Wright,[1] and James R. Cox[2,3]
[1]Antimicrobial Research Centre
Department of Biochemistry
McMaster University
1200 Main Street West
Hamilton, Ontario, L8N 3Z5
Canada
[2]Department of Chemistry
Murray State University
456 Blackburn Science Building
Murray, Kentucky 42071

Summary

A key contact in the active site of an aminoglycoside phosphotransferase enzyme (APH(3′)-IIIa) is a π-π stacking interaction between Tyr42 and the adenine ring of bound nucleotides. We investigated the prevalence of similar Tyr-adenine contacts and found that many different protein systems employ Tyr residues in the recognition of the adenine ring. The geometry of these stacking interactions suggests that electrostatics play a role in the attraction between these aromatic systems. Kinetic and calorimetric experiments on wild-type and mutant forms of APH(3′)-IIIa yielded further experimental evidence of the importance of electrostatics in the adenine binding region and suggested that the stacking interaction contributes ~2 kcal/mol of binding energy. This type of information concerning the forces that govern nucleotide binding in APH(3′)-IIIa will facilitate inhibitor design strategies that target the nucleotide binding site of APH-type enzymes.

Introduction

Noncovalent interactions play vital roles in many aspects of chemistry and biology, and consequently, various types of experimental and theoretical approaches have been used to study these forces [1]. Special attention has been placed on interactions involving aromatic systems (π-π interactions) since they play important roles in the stabilization of macromolecular structures involving nucleic acids, proteins, and materials such as liquid crystal copolymers [2–9].

Some of the most significant π-type interactions may be found in protein complexes involving ligands with purine- and pyrimidine-type ring systems. There is a diverse set of large and small molecules that contain these types of rings and make biologically important complexes with proteins. For example, studies have clearly demonstrated the prevalence of π-π stacking interactions in complexes involving proteins and nucleic acids, most notably single-stranded RNA [10–15]. Furthermore, there have been numerous other reports of π-π stacking interactions in protein complexes involving ligands (other than DNA/RNA) containing the adenine and guanine ring [16–23]. This seems to be in contrast with a report that downplayed the involvement of aromatic amino acids in the packing of the adenine ring in protein structures [24].

A prominent example of such a π-π interaction involving an aromatic amino acid and an adenine ring can be found in an aminoglycoside antibiotic 3′,5″-phosphotransferase (APH(3′)-IIIa). Scrutiny of the nucleotide binding site of the enzyme reveals there are three major contacts with the adenine ring of bound ADP. This includes a π-π stacking interaction involving Tyr42 and two hydrogen bonding interactions with backbone atoms of Ser91 and Ala93 (Figure 1) [18, 25]. APH(3′)-IIIa belongs to a family of aminoglycoside antibiotic kinases that phosphorylate various hydroxyl groups around the aminoglycoside structure [26–29]. Phosphorylated antibiotic does not bind efficiently to its target, the bacterial ribosomal aminoacyl-tRNA site of the 16S RNA, resulting in a resistance phenotype in organisms harboring the aminoglycoside phosphotransferases [30].

One approach to returning efficacy to aminoglycosides in resistant organisms is to coadminister potent and specific inhibitors of APHs with the antibiotics, allowing the drug to bypass the resistance mechanism [31]. A thorough analysis of the specific binding opportunities and energies available in APHs, specifically the enterococcal and staphylococcal resistance determinant APH(3′)-IIIa, will be beneficial toward the development of potent inhibitors. This is very important considering that APH(3′)-IIIa is structurally similar to Ser/Thr/Tyr protein kinases [18]. Moreover, the structural homology translates into functional similarity in that APHs can phosphorylate peptides [32], and in that APHs and protein kinases likely have similar catalytic mechanisms [33, 34]. Not surprisingly then, among the first generation of APH inhibitors [35–38] include compounds that also act as protein/lipid kinase inhibitors [39, 40]. However, to minimize host toxicity, inhibitors of APHs should not be cross-reactive with eukaryotic protein kinases. Thus, the identification and understanding of the differences in the active sites between protein kinases and APHs are critical to developing specific inhibitors of aminoglycoside kinases, especially if directed against the nucleotide binding pocket.

It has been previously noted that the π-π stacking arrangement observed in the crystal structures of APH(3′)-IIIa complexed with ADP and the nonhydrolyzable ATP analogue AMPPNP is not shared with the protein kinase family, where an alanine is at the equivalent position [25]. In the structure of APH(3′)-IIIa, the presence of Tyr42 causes the adenine ring to be turned 40° relative to its counterparts in the protein kinases. Thus, considering that the π-π stacking arrangement is conserved in the APH(3′) family of enzymes (either Tyr or Phe at this position) but is lacking in protein kinases, taking advantage of this interaction in the design of

[3]Correspondence: ricky.cox@murraystate.edu

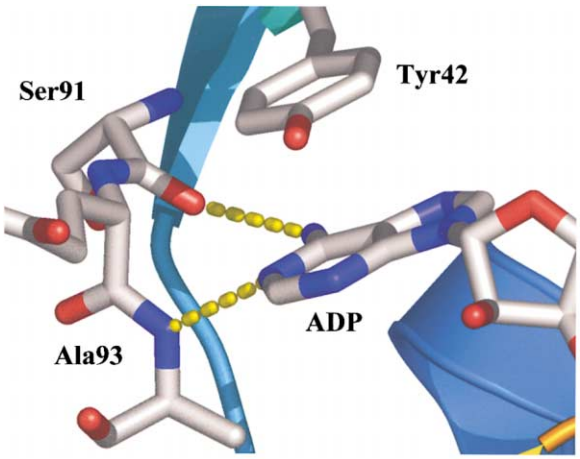

Figure 1. The Adenine Binding Pocket in the Active Site of APH(3′)-IIIa

The three major contacts with the adenine ring of the bound nucleotide are presented. H bonds are represented by the dashed yellow lines and are drawn between the amide group of Ala93 and N1 of the adenine ring and the carbonyl group of Ser91 and the amino group at position 6 of the adenine ring. Hydrogen atoms have been omitted for clarity. The π-π stacking interaction between Tyr42 of the enzyme and the bound nucleotide is also shown. A standard CPK color scheme has been used where carbons are gray, oxygens are red, and nitrogens are blue. This figure was generated in the program PyMol (http://pymol.sourceforge.net/).

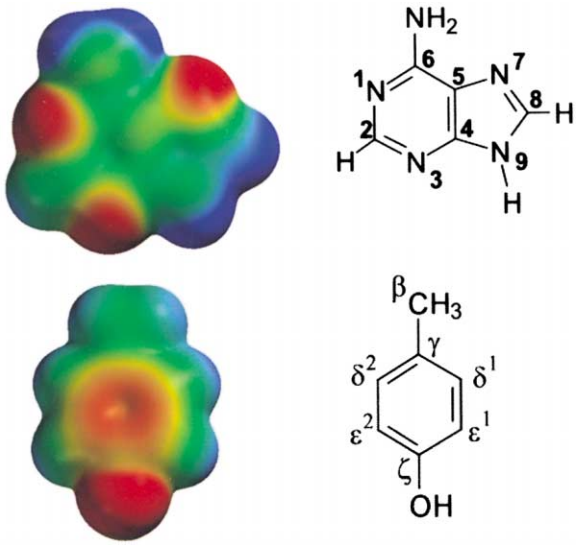

Figure 2. Electrostatic Potential Maps of Important Aromatic Systems

The electrostatic potential maps of adenine (top) and *p*-hydroxytoluene (bottom) calculated at the HF/6-311G* level of theory. The structure of each molecule is provided on the right for reference. The numbering of *p*-hydroxytoluene is based on the side chain of Tyr and was adopted from Creighton [72]. The potential energy extremes are −25 to +25 kcal/mol. The color red indicates areas of greater electron density, while blue indicates areas of less electron density. From negative to positive potentials, the colors progress red-orange-yellow-green-cyan-blue.

inhibitors will provide some measure of specificity towards aminoglycoside kinases. Understanding the magnitude and the nature of the energy involved in this interaction will allow us to design compounds that maximize this discriminating binding opportunity. APH(3′)-IIIa can also then serve as a point of reference when examining aromatic protein-ligand interactions in other protein complexes.

In this report, we provide a survey of the interaction of Tyr side chains with the adenine ring of bound ligands in protein complexes. This frequency data has allowed us to compare the π-π stacking interaction observed in APH(3′)-IIIa to other similar stacking interactions. In addition, to probe the Tyr42-adenine contact in APH(3′)-IIIa, Tyr42 mutants have been analyzed both in terms of their effects on enzyme activity, and the enthalpic and entropic contributions to binding energy using isothermal titration calorimetry.

Results and Discussion

Electrostatic Potential Surfaces of Adenine and *p*-Hydroxytoluene

To gain a better perspective on the Tyr-adenine contact in APH(3′)-IIIa, we wanted to understand the electronic factors associated with the stacking interaction and to compare similar interactions in other protein complexes. Towards the first goal, the electrostatic potential surfaces of adenine and *p*-hydroxytoluene were calculated using quantum mechanical methods (Figure 2). The electrostatic map of adenine indicates that most of the negative charge is centered around N1, N3, and N7 and the positive charge is on hydrogens bound to nitrogen atoms or sp^2-hybridized carbon atoms. The calculation and electrostatic map of adenine also suggests that N9 is less electronegative compared to the other heterocyclic nitrogen atoms. Other calculations on adenine derivatives (data not shown) also suggest that whether a hydrogen atom, $-CH_2-$, or $-CH_3$ group is attached to N9, these substituents lead to an electropositive region. This can be visualized in the electrostatic potential surface of adenine in Figure 2, with a hydrogen atom bonded to N9. These results are in qualitative agreement with previous electronic studies on the adenine ring system [41]. The electrostatic potential surface of *p*-hydroxytoluene (Figure 2) illustrates the charge distribution in the Tyr side chain, where most of the negative charge is distributed on the electronegative oxygen atom and in the body of the aromatic ring. This surface is similar to that generated through previous quantum-mechanical calculations on phenol [42].

Frequency and Nature of Tyrosine-Adenine Stacking Interactions in Protein Complexes

To place the stacking interaction in APH(3′)-IIIa in context with other similar interactions, the Protein Data Bank was searched to establish the frequency and nature of these types of interactions. Overall, 281 protein complexes that contain an adenine-bearing ligand were identified and investigated. Including APH(3′)-IIIa, a total of 34 unique complexes were recognized as having a Tyr residue in the vicinity of an adenine moiety. The categorization of π-π stacking interactions can be somewhat subjective; therefore, any Tyr residue nearly parallel to the adenine ring was included in the analysis. The following is a list of the diverse set of ligands in these 34 complexes and the number of examples found

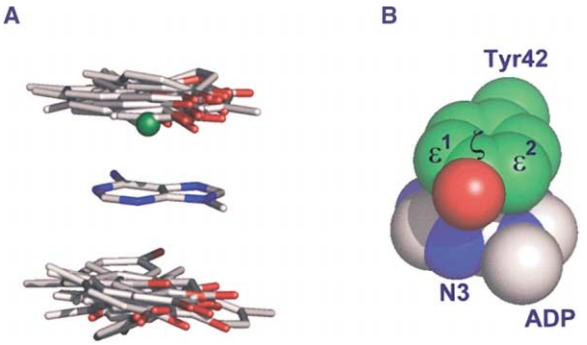

Figure 3. π-π Interactions in Protein Complexes

(A) The overlay of the Tyr-adenine model systems generated from 34 protein coordinate files and deleting all of the atoms except for the two aromatic rings is shown. All of the model systems were superimposed at the adenine ring, and hydrogens are not shown for clarity. A total of 35 Tyr residues are shown as one coordinate file (1AMO) contained two stacking interactions. A standard CPK color scheme has been used where carbons are gray, oxygens are red, and nitrogens are blue. The oxygen atom of Tyr42 in APH(3′)-IIIa is shown as a green sphere. The B face of the adenine ring is above the plane of the ring and the A face is below the plane of the ring [43]. The PDB codes used to construct the model systems include: 1DGY, 1QD2,1QG0, 1QGX, 1YKF,1QKI, 1FA9, 1AMO, 1CNF, 1PFK, 1QCI, 1G18, 1MAB, 1IFS, 1DDG, 1J7L, 1MRG, 1EWY, 1B0U, 1A0I, 1EFR, 1E19, 1DQA, 1CXY, 1QHG, 1DGS, 1D9Z, 1ECJ, 1FNB, 1QUE, 8GPB, 1E0J, 1CR2, and 1G6O.

(B) A zoomed view of the π-π stacking interaction between Tyr42 and the adenine ring of ADP in the active site of APH(3′)-IIIa. The carbon atoms of Tyr42 are green; otherwise, a standard CPK color scheme has been used. The numbering of the Tyr side chain was adopted from Creighton [72]. This figure was generated from the coordinates of the APH(3′)-IIIa-ADP complex (PDB code: 1J7L) and removing all the atoms except for the interacting rings. The images in this figure were generated in the program PyMol (http://pymol.sourceforge.net/).

with each: adenine (5), adenosine (1), FAD (6), ATP (5), dATP (1), ADP (6), AMP (5), cAMP (1), and $NADP^+$ (5). In NADH:Cytochrome P450 Reductase (1AMO), two different Tyr residues are stacking against the adenine ring of FAD and $NADP^+$. Overall, there were a total of 35 stacking interactions in the 34 protein complexes. The results of this survey suggest that π-π stacking interactions involving aromatic amino acids and the adenine ring are important contacts and cannot be ignored when dissecting the adenine binding region of proteins.

Model systems of the Tyr-adenine interactions were constructed using the coordinate files of the 34 protein complexes. Each of the model systems contained only the Tyr residue (represented as *p*-hydroxytoluene) and N9-methyladenine or adenine. The model systems were superimposed at the adenine ring, and the overlay is presented in Figure 3A. The faces of the adenine ring can be designated as A or B, depending on whether the numbering of the ring progresses in a clockwise or counterclockwise direction, respectively [24, 43]. Of the 35 stacking interactions, 17 were at the A face and 18 were at located at the B face of the adenine ring. In the orientation presented in Figure 3A, the B face is above the plane of the ring, and the A face is below the plane of the ring.

The arrangements of Tyr side chains in Figure 3 are similar in that most of the rings are in a region of space above or below the adenine ring. It is also clear that some of the 35 interactions can be described as traditional π-π stacking interactions, while others may not deserve that description because of a slight tilted orientation. All of the Tyr side chains in the vicinity of an adenine ring were retained because we were also interested in the distribution of Tyr side chain oxygen atoms relative to the adenine ring. The clustering of the Tyr oxygen atoms in the overlay was striking and unexpected. Most of the oxygen atoms are outside the plane of the adenine ring and project to a region near N9 or the atom attached to this nitrogen atom, especially on the B face. According to the electrostatic potential map of adenine (Figure 2), and previous calculations on the adenine ring system [41], this is one of the least electronegative regions of the adenine ring. Having the electronegative oxygen atom of Tyr project away from highly electronegative regions of the adenine ring (such as N1, N3, and N7) avoids charge-charge repulsions in the stacking interaction. As mentioned previously, there is significant π electron density in the phenolic side chain of Tyr. This correlates well with the fact that many of the Tyr side chains have aromatic rings that are positioned such that they also avoid the highly electronegative regions of the adenine ring in the stacking interactions (Figure 3A).

The stacking interaction in the active site of APH(3′)-IIIa is rather distinctive from the other stacking interactions, as indicated by the green sphere in Figure 3A. This sphere is the oxygen atom of Tyr42 and is at the periphery of the cluster of oxygen atoms at the B face and is projected more toward N3 of the adenine ring. A closer view of the stacking interaction in APH(3′)-IIIa (Figure 3B) reveals that the two rings are coplanar (also see Figure 1) and the distances between the oxygen atom of Tyr42 and N3 and N9 of the adenine ring system are 3.52 and 4.38 Å, respectively. In addition, the distances between ϵ^1, ϵ^2, and ζ carbons of the Tyr ring and N3 are 3.49, 3.89, and 3.37 Å, respectively. As the body of the aromatic ring and the electronegative oxygen of Tyr42 is projected more toward N3 (Figure 3B), which is one of the most electronegative regions of the adenine ring, it is reasonable to expect there may be an element of electrostatic repulsion in the arrangement of the Tyr-adenine contact and lead to a partial destabilization of the APH(3′)-IIIa-ADP complex. In other words, the fact that the two electronegative atoms are close to each other may make the interaction between the aromatic systems less attractive compared to other possible orientations observed in Tyr-adenine stacking contacts. An extremely tight complex between ADP and APH(3′)-IIIa would put the enzyme at a catalytic disadvantage because release of ADP is the last and rate-determining step in the phosphorylation of aminoglycoside antibiotics. Thus, electrostatic considerations seem to play a role in aligning the adenine ring with the phenolic side chain of Tyr in the stacking interactions identified in this study.

Kinetic and Thermodynamic Analyses of the π-π Stacking Interaction between APH(3′)-IIIa and Nucleotide Ligands

To investigate the nature of the π-π interaction in the nucleotide binding site of APH(3′)-IIIa, we produced mu-

Table 1. Kinetic Analyses of APH(3′)-IIIa Wild-Type and Tyr42 Mutants

	K_M (μM)	k_{cat} (s^{-1})	k_{cat}/K_M ($M^{-1}s^{-1}$)	K_M^{mut}/K_M^{wt}	$k_{cat}^{wt}/k_{cat}^{mut}$	$(k_{cat}/K_M)^{wt}/(k_{cat}/K_M)^{mut}$
APH(3′)-IIIa wt[a]						
ATP[b]	27.7 ± 3.7	1.76 ± 0.08	6.35×10^4	–	–	–
Kanamycin A[c]	12.6 ± 2.6	1.79 ± 0.08	1.42×10^5	–	–	–
Neomycin B[c]	7.72 ± 0.9	2.08 ± 0.07	2.69×10^5	–	–	–
APH(3′)-IIIa Tyr42Phe						
ATP[b]	6.31 ± 0.57	0.34 ± 0.01	5.32×10^4	0.23	5.2	1.2
Kanamycin A[c]	8.74 ± 2.6	0.36 ± 0.02	4.08×10^4	0.69	5.0	3.5
Neomycin B[c]	13.8 ± 1.6	1.54 ± 0.05	1.11×10^5	1.8	1.4	2.4
APH(3′)-IIIa Tyr42Val						
ATP[b]	272 ± 23	2.93 ± 0.07	1.08×10^4	9.8	0.60	5.9
Kanamycin A[d]	3.56 ± 1.29	2.70 ± 0.14	7.59×10^5	0.28	0.66	0.19
Neomycin B[d]	6.93 ± 1.68	1.87 ± 0.10	2.70×10^5	0.90	1.1	1.0

[a] Kinetic parameters for ATP taken from [18], whereas those for aminoglycoside substrates taken from [26].
[b] Parameters determined in the presence of 125 μM kanamycin A.
[c] Parameters determined in the presence of 1 mM ATP.
[d] Parameters determined in the presence of 3 mM ATP.

tant proteins Tyr42Ala, Tyr42Phe, and Tyr42Val. APH(3′)-IIIa Tyr42Ala was insoluble (data not shown) and could not be used in the study. This indicates that Tyr42 may be important in the proper folding of the enzyme. Proteolysis studies of the mutant Tyr42Val and Tyr42Phe proteins with subtilisin yielded the same fragment pattern as APH(3′)-IIIa wt protein (data not shown), suggesting that there are no gross alterations in protein structure with these mutant proteins. Furthermore, the far-UV circular dichroism (CD) spectra for APH(3′)-IIIa wt and APH(3′)-IIIa Tyr42Val (data not shown) are essentially identical, verifying that proper secondary structure is maintained upon mutation of Tyr42. Together, these results suggest that there are no significant structural differences between APH(3′)-IIIa wt and Tyr42Phe and Tyr42Val proteins.

Kinetic Analyses

APH(3′)-IIIa follows a special form of an ordered BiBi kinetic mechanism in the steady state known as Theorell-Chance [27, 44], where the Michaelis-Menten constant (K_M) for ATP closely approximates the dissociation constant (K_D) for ATP. Thus, for APH(3′)-IIIa, K_M for ATP gives a true dissociation constant and can be used as a measure of nucleotide affinity for the protein. Furthermore, ADP departure is rate limiting, and so, tighter binding of nucleotide may result in a slower release of ADP and a decrease in the overall rate (k_{cat}).

APH(3′)-IIIa Tyr42Phe appeared to bind ATP more tightly than wild-type enzyme, where K_M for ATP decreased 4-fold compared to wt enzyme (Table 1). The apparent affinities for the aminoglycosides kanamycin A and neomycin B were less affected by the mutation, where the changes in K_M were less than two-fold. The tighter binding of nucleotide (ATP/ADP) is reflected in the decrease in k_{cat} (1.4- to 5.2-fold; Table 1).

The mutation of Tyr42Val had a much more dramatic effect on the affinity for ATP, where K_M for ATP increased nearly 10-fold (Table 1). The affinity for ADP was likely decreased as well considering the modest increase in k_{cat} (2-fold), despite an overall decrease in the catalytic efficiency (k_{cat}/K_M; 5.9-fold). The K_M values for the 4,6-disubstituted aminoglycoside kanamycin A, but not the 4,5-disubstituted neomycin, is reduced modestly in the Tyr42Val mutant compared to the wt and Tyr42Phe enzymes. Unlike ATP, the K_M for aminoglycosides is a complex function of several rate constants, and this slight change in value is not likely attributable to a change in K_D, especially as the amino acid is remote from the aminoglycoside binding site and there is no comparable effect on neomycin K_M.

Thermodynamic Analyses

The thermodynamics of the interaction between APH(3′)-IIIa and nucleotide ligand can be investigated directly through isothermal titration calorimetry (ITC). ITC measures the heat exchanged with the environment upon association between a receptor and a ligand. Thus, ITC directly measures the enthalpy of binding (ΔH), and a titration of the binding sites will yield an association constant (K_A). Using these two values, we can obtain a complete thermodynamic profile of the interaction using the formula $-RT \ln K_A = \Delta G = \Delta H - T\Delta S$.

As K_M for ATP closely approximates K_D for ATP, we can get an estimate of the Gibbs free energy of ATP binding (Table 2). These values are very comparable to those values for the Gibbs free energy of ADP binding using ITC (Figure 4; Table 2). From the ITC experiments, it can be seen that ADP binding to APH(3′)-IIIa wt is dominated by enthalpic forces, whereas the entropic contribution is unfavorable (Table 2). Similarly, binding of ADP to APH(3′)-IIIa Tyr42Phe is governed by enthalpy and entropy is unfavorable; however, enthalpy is slightly less favorable and entropy is slightly more favorable with the Tyr42Phe mutant protein compared to wt (Figure 5).

This result may seem counterintuitive to the argument presented before where electrostatic repulsion may exist in the Tyr42-adenine stacking interaction. On the other hand, the crystal structure of the APH(3′)-IIIa-ADP complex shows several water molecules in the vicinity of the hydroxyl group on Tyr42 and N3 of the adenine ring [25]. A hydrogen bonding network in this area will help support the stacking interaction and the binding of nucleotide to the enzyme. Upon mutation to Phe at position 42, the electrostatic repulsion in the stacking interaction would be diminished, but the hydrogen bonding network would also be partially disrupted. Taken together, this will lead to an overall negative ΔΔH

Table 2. Thermodynamic Parameters for Nucleotide Binding to APH(3′)-IIIa Wild-Type and Tyr42 Mutants

	ATP[a,b]		ADP[c]			
	K_D (μM)	ΔG (kcal/mol)	K_D (μM)	ΔH (kcal/mol)	−TΔS (kcal/mol)	ΔG (kcal/mol)
Wild-Type	27.7 ± 3.7	−6.46	17.06 ± 2.60	−11.52 ± 0.5	+4.90	−6.62
Tyr42Phe	6.31 ± 0.57	−7.38	6.46 ± 0.28	−10.20 ± 0.2	+3.00	−7.20
Tyr42Val	272 ± 23	−5.06	186.7 ± 25.7	−1.95 ± 0.2	−3.22	−5.17

[a] The values determined in 50 mM HEPES-NaOH (pH 7.5), 40 mM KCl, 10 mM $MgCl_2$.
[b] In APH(3′)-IIIa, the K_M for ATP approximates K_D for ATP [27], so ΔG was calculated according to $\Delta G = -RT \ln (1/K_D)$, where T = 310 K in the kinetic assays.
[c] Parameters for ADP were determined using ITC at 303 K as described in Experimental Procedures.

value for the mutant and suggests that enthalpy has become less favorable toward nucleotide binding (Figure 5). Also, a partial loss of the hydrogen bonding interactions may lead to greater flexibility of the bound nucleotide in this region and result in a positive ΔΔS value for this mutant with respect to ADP binding (Figure 5).

In contrast to the results for APH(3′)-IIIa wt and Tyr42-Phe, the entropy contribution is favorable for Tyr42Val and is most responsible for the interaction with ADP, although enthalpy still makes an important contribution (Table 2; Figure 5). Molecular modeling on the nucleotide binding site of APH(3′)-IIIa (data not shown) has revealed

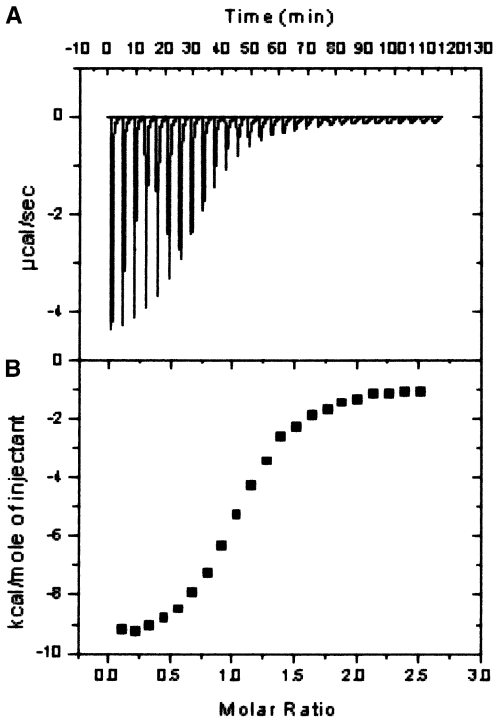

Figure 4. Isothermal Calorimetric Titration for the Interaction between ADP and APH(3′)-IIIa

(A) Raw data for 22 10 μl injections of ADP (2.0 mM stock) into the isothermal cell containing 100 μM APH(3′)-IIIa wt at 4 min intervals and 30°C. Both the protein and ADP were in 50 mM HEPES-NaOH (pH 7.5), 40 mM KCl, and 10 mM $MgCl_2$.

(B) Experimental points were obtained by the integration of the above peaks and plotted against the molar ratio of ADP to protein in the reaction cell.

that replacing Tyr with Val at position 42 should not hinder the nucleotide from entering the adenine binding region or making hydrogen bonding contacts with the backbone atoms of Ser91 and Ala93. In addition, the mutation to Val makes the adenine binding region more hydrophobic, an environment common to the binding of the adenine ring in other protein complexes [24]. Our results with the Tyr42Val mutant suggest that the binding of ADP is entropically driven, which is to be expected when binding is mostly hydrophobic or dispersive in nature [45]. However, in the case of APH(3′)-IIIa, having a more hydrophobic nucleotide binding pocket (as in the Tyr42Val mutant) compromises nucleotide affinity. This result highlights the importance of polar interactions in the association of an aromatic amino acid in position 42 and the adenine ring and the difference between the nucleotide binding pocket of APH(3′)-IIIa and those of other similar ATP binding proteins, including Ser/Thr protein kinases. These discrete requirements for high-affinity binding to APH(3′)-IIIa and the conservation of the Tyr residue among six of the APH-class enzymes [46] provides the structural and energetic leverage for the development of ATP-site-directed inhibitors specific for APH enzymes.

Comparison to Other Stacking Interactions

Previous studies have addressed the energy associated with the stacking of an aromatic amino acid with a nucleobase in RNA. RNA-protein complexes have been destabilized 3.0–5.5 kcal/mol (ΔΔG values) upon mutation of the aromatic side chain to Ala [15, 47, 48]. Experimental and theoretical studies on nucleic acid base stacking in DNA and RNA have estimated the stacking of two nucleobases in these structures contribute no more than 4.0 kcal/mol (ΔΔG values) of stabilization [5, 49, 50]. Model calculations on benzene and toluene dimers (parallel and off center) have yielded interaction energies (gas phase and aqueous solution) for these systems to be in the range of 1.0–4.0 kcal/mol [51, 52].

In APH(3′)-IIIa, the thermodynamic parameters associated with ADP binding to the Tyr42Phe and Tyr42Val mutants should be a good measure of the energy lost upon removing the stacking interacting (Table 2). The ΔΔG value associated with these two mutants is 2.03 kcal/mol, which is in the range of energies given above. This number can only be used as a qualitative guide as there may be some dispersive-type interactions between the isopropyl side chain of Val and the adenine

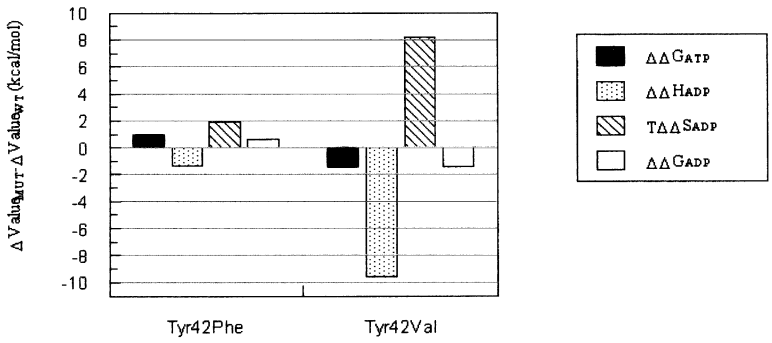

Figure 5. Thermodynamic Analysis of Nucleotide Binding to APH(3′)-IIIa Mutants

Changes in the thermodynamic contributions to nucleotide binding upon mutation of APH(3′)-IIIa Tyr42 are based on the values in Table 2. Plotted values are relative to wt (i.e., $\Delta\Delta Value = \Delta Value_{MUT} - \Delta Value_{wt}$); thus, positive values indicate that the thermodynamic parameter is more favorable in the mutant compared to wt.

ring in the Tyr42Val mutant. Since the free energy values presented in other studies are not broken down into enthalpic and entropic contributions, a more detailed comparison is not possible.

The fundamental forces that govern π-π interactions are widely debated, with some studies highlighting polar or electrostatic (dipolar/quadrupolar) contributions, while others point to the importance of hydrophobic effects and dispersion forces [1, 5, 8, 50–67]. Many of the previous studies have used experimental approaches employing model systems or theoretical calculations on such systems as the benzene dimer or stacked nucleobases. For example, a recent study using carefully designed model systems concluded that polar interactions play an important role in heteroaromatic-(hetero)aromatic attractions in water [56]. The results of this study have implications in nucleic acid base stacking and provide an interesting comparison to our finding that polar interactions play a role in stacking interactions involving aromatic amino acids and the heteroaromatic adenine ring.

When placing our results in context with previous studies in the vast arena of π-π interactions, we believe that it is important to note that we are commenting on a class of interactions that have been observed in biologically important protein complexes. We have also shown that the cataloging of different types of π-π interactions and analysis of their geometry need to accompany studies to investigate their nature and energetics. The reason that a theory unifying the nature of π-π interactions has not emerged may be due to the fact that the formation of specific types of π-π interactions is governed by different factors or a combination of different factors that contribute to their stability. Our conclusion that electrostatics are important in Tyr/Phe-adenine stacking interactions may only be applicable to this subset of biological π-π interactions. Therefore, the diversity of π-π interactions found in biological molecules will certainly demand that specific examples be cataloged and investigated to fully understand their ability to help stabilize macromolecular structures.

Significance

It is becoming clear that π-π interactions are important components in the structural architecture of many types of biological molecules. The nature of the interaction has been described as primarily electrostatic or primarily hydrophobic and dispersive depending on the system in question. As the stabilizing forces may be interaction specific, it is informative to provide a diverse range of examples. An understudied area is the π-π interactions found in protein-ligand complexes where the aminoglycoside resistance enzyme APH(3′)-IIIa provides an important example. Our approach is unique in that we combine a survey of Tyr-adenine stacking contacts in protein complexes with calorimetric studies to probe the energetics of such interactions. The survey of Tyr-adenine interactions indicates that stacking interactions are used by a variety of protein systems to recognize adenine-bearing ligands. The geometry of these interactions suggests that polar or electronic forces play an important role in the interplay of these aromatic systems. In the case of APH(3′)-IIIa, this finding is further supported by our mutation studies where a thermodynamic analysis with wild-type and mutant forms of the enzyme indicates that the π-π stacking interaction provides an electrostatic contribution to nucleotide binding, where the stacking interaction provides up to 2 kcal/mol toward stabilization of the complex. Moreover, these results suggest that high-affinity interaction with the adenine binding pocket of APH(3′)-IIIa will require the proper electrostatic complementation to the protein. This is in contrast to other nucleotide binding proteins including the structurally similar Ser/Thr/Tyr protein kinases, where the adenine binding pockets are mostly hydrophobic and binding interactions would be predicted to be dispersive in nature. As Tyr42 is conserved among most APH proteins, this unique feature of APHs provides the structural basis for the design of APH-specific inhibitors, which could reverse antibiotic resistance in vivo.

Experimental Procedures

Chemicals

Neomycin B, ATP, β-NADH, phosphoenol pyruvate, and PK/LDH enzymes were from Sigma (St. Louis, MO). Kanamycin A was from Bioshop (Burlington, ON, Canada). Oligonucleotide primers were purchased from the Central Facility of the Institute for Molecular Biology and Biotechnology, McMaster University.

Ab Initio Calculations on Adenine and *p*-Hydroxytoluene

Adenine and *p*-hydroxytoluene were constructed and underwent geometry optimization using the HF/6-311G** level of theory. Electrostatic potential surfaces were generated by mapping the 6-311G** potentials onto surfaces of molecular electron density. The potential energy extremes shown in Figure 2 are −25 to +25 kcal/mol. The areas in red represent negative electrostatic potentials, and the areas in blue represent positive potentials. All calculations were

performed in Spartan '02 (Wavefunction, Inc., Irvine, CA) running on a SGI Octane Workstation.

Searching the Protein Data Bank

To investigate the frequency of Tyr-adenine interactions, the Protein Data Bank (PDB), housed at The Research Collaboratory for Structural Bioinformatics (http://www.rcsb.org) [68], was searched using ReliBase (http://relibase.ccdc.cam.ac.uk) [69], a program designed to identify protein-ligand complexes. Search terms in ReliBase included such words as adenine, adenosine, and adenosine triphosphate. Overall, 281 protein complexes that contained a ligand with an adenine ring (other than RNA/DNA) were derived from the analysis and visualized in Protein Explorer (http://www.proteinexplorer.org) [70]. Tyr residues in the vicinity of an adenine ring in the protein complexes were highlighted and underwent further investigation if the two rings were nearly parallel and no longer than 4 Å apart. Model systems of these interactions were generated by downloading the coordinate files from the Protein Data Bank. The interacting rings were identified, and the remaining atoms in the coordinate file were removed. Hydrogen atoms were added to the rings and used to fill open valences, which created methyl derivatives of the aromatic ring systems, except when adenine itself was the ligand. It is important to note that the model systems resulting from this method have the aromatic rings in the exact geometry as found in the crystal structures. The model systems were superimposed at the adenine ring to investigate the distribution of Tyr side chains around the adenine ring in protein complexes.

Site-Directed Mutagenesis

Tyr42 mutants were generated using the QuikChange mutagenesis protocol (Stratagene, La Jolla, CA) using appropriate primers. All mutant genes were sequenced in their entirety at the Central Facility of the Institute for Molecular Biology and Biotechnology, McMaster University, to ensure that undesired mutations had not been incorporated during the PCR reactions.

Purification of Mutant APH(3′)-IIIa Proteins

The purification of APH(3′)-IIIa overexpressed from *Escherichia coli* BL21(DE3)/pETSACG1 has previously been described [26], and the purification of mutant proteins followed a similar procedure.

Kinetic Assay

The kinetic assay used to monitor APH(3′) activity has been previously described [26]. For this study, the reaction volumes were scaled down from 1 ml to 250 μl so the assays could be conducted in 96-well microtitre plates using a Molecular Devices SpectraMax Plus plate reader. The assay measures the production of ADP generated upon aminoglycoside phosphorylation and couples that production to the oxidation of β-NADH using the enzymes pyruvate kinase and lactate dehydrogenase. The rate of ADP production was thus determined by monitoring the decrease in absorbance at 340 nm. Initial rates were fit by nonlinear least square methods to Equation 1,

$$v = k_{cat}E_t[S]/(K_M + [S]), \quad (1)$$

or Equation 2,

$$v = k_{cat}E_t[S]/(K_M + [S])(1 + [S]/K_i), \quad (2)$$

if substrate inhibition was detected using Grafit version 4.0 (Erithacus Software, Ltd., Staines, UK), where v is the initial velocity, E_t is the total amount of enzyme present, and [S] is the concentration of substrate.

Isothermal Titration Calorimetry

All of the ITC experiments were performed on a VP-ITC from Microcal Inc. (Northampton, MA). The experiments were conducted at 30°C in APH assay buffer that includes 50 mM HEPES-NaOH, pH 7.5, 40 mM KCl, and 10 mM $MgCl_2$. The proteins were dialyzed completely against buffer, and the buffer was used to dissolve ADP. The ADP solution was readjusted to pH 7.5 with a small amount of NaOH. The protein concentration in the sample cell of the calorimeter was 100–300 μM, and the ADP concentration in the syringe was 2 mM. The volume of the individual injection was 10 μl set at a syringe rate of 0.5 μl/s. A time period of 240 s was allowed between each injection for recovery back to baseline, and the stirring speed was set at 300 rpm. The experimental titrations were corrected for by subtracting the heat of dilution for ADP into buffer. The heat of dilution for the protein was found to be negligible. The binding data was then analyzed using Origin software [71]. The binding constant (K) and the enthalpy change (ΔH) were used to calculate the free energy change (ΔG), and the entropy change (ΔS) according to the relations in Equation 3.

$$-RT \ln K = \Delta G = \Delta H - T\Delta S \quad (3)$$

Acknowledgments

This research was supported by the Canadian Institutes of Health Research (MT-13536), a Howard Hughes Medical Institute Undergraduate Biological Sciences Education grant to Murray State University, and the Kentucky National Science Foundation EPSCoR program (REG grant to J.R.C.). Support of the National Institutes of Health and the National Center for Research Resources Grant (P20-RR16481), which established the Kentucky Biomedical Research Infrastructure Network, is also acknowledged. G.D.W. holds a Canada Research Chair in Antibiotic Biochemistry.

Received: July 18, 2002
Revised: September 3, 2002
Accepted: September 24,2002

References

1. Müller-Dethlefs, K., and Hobza, P. (2000). Noncovalent interactions: a challenge for experiment and theory. Chem. Rev. *100*, 143–167.
2. Burley, S.K., and Petsko, G.A. (1985). Aromatic-aromatic interaction: a mechanism of protein structure stabilization. Science *229*, 23–28.
3. Kool, E.T., Morales, J.C., and Guckian, K.M. (2000). Mimicking the structure and function of DNA: insights into DNA stability and replication. Angew. Chem. Int. Ed. Engl. *39*, 990–1009.
4. Hunter, C.A., Singh, J., and Thornton, J.M. (1991). π-π interactions: the geometry and energetics of phenylalanine-phenylalanine interactions in proteins. J. Mol. Biol. *218*, 837–846.
5. Guckian, K.M., Schweitzer, B.A., Ren, R.X.-F., Sheils, C.J., Tahmassebi, D.C., and Kool, E.T. (2000). Factors contributing to aromatic stacking in water: evaluation in the context of DNA. J. Am. Chem. Soc. *122*, 2213–2222.
6. Serrano, L., Bycroft, M., and Fersht, A.R. (1991). Aromatic-aromatic interactions and protein stability. J. Mol. Biol. *218*, 465–475.
7. McGaughey, G.B., Gagne, M., and Rappé, A.K. (1998). π-stacking interactions: alive and well in proteins. J. Biol. Chem. *271*, 15458–15463.
8. Heaton, N.J., Bello, P., Herradón, B., del Campo, A., and Jiménez-Barbero, J. (1998). NMR study of intramolecular interactions between aromatic groups: van der waals, charge-transfer, or quadrupolar interactions? J. Am. Chem. Soc. *120*, 9632–9645.
9. Kirksey, T.J., Pogue-Caley, R.R., Frelinger, J.A., and Collins, E.J. (1999). The structural basis for the increased immunogenicity of two HIV-reverse transcriptase peptide variant/class I major histocompatibility complexes. J. Biol. Chem. *274*, 37259–37264.
10. Ohndorf, U.-M., Rould, M.A., He, Q., Pabo, C.O., and Lippard, S.J. (1999). Basis for recognition of cisplatin-modified DNA by high-mobility-group proteins. Nature *299*, 708–712.
11. Valegard, K., Murray, J.B., Stonehouse, N.J., van den Worm, S., Stockley, P.G., and Liljas, L. (1997). The three-dimensional structures of two complexes between recombinant MS2 capsids and RNA operator fragments reveal sequence-specific protein-RNA interactions. J. Mol. Biol. *270*, 724–738.
12. Oubridge, C., Ito, N., Evans, P., Teo, C.-H., and Nagal, K. (1994). Crystal structure at 1.92 Å resolution of the RNA-binding domain of the U1A spliceosomal protein complexed with an RNA hairpin. Nature *372*, 432–438.

13. Price, S.R., Evans, P.R., and Nagal, K. (1998). Crystal structure of the spliceosomal U2B″-U2A′ protein complex bound to a fragment of U2 small nuclear RNA. Nature *394*, 645–650.
14. Handa, N., Nureki, O., Kurimoto, K., Kim, I., Sakamoto, H., Shimura, Y., Muto, Y., and Yokoyama, S. (1999). Structural basis for recognition of the *tra* mRNA precursor by the sex-lethal protein. Nature *398*, 579–585.
15. Nolan, S.J., Shiels, J.C., Tuite, J.B., Cecere, K.L., and Baranger, A.M. (1999). Recognition of an essential adenine at a protein-RNA interface: comparison of the contributions of hydrogen bonds and a stacking arrangement. J. Am. Chem. Soc. *121*, 8951–8952.
16. Rath, V.L., Ammirati, M., LeMotte, P.K., Fennell, K.F., Mansour, M.N., Danley, D.E., Hynes, T.R., Schulte, G.K., Wasilko, D.J., and Pandit, J. (2000). Activation of human liver glycogen phosphorylase by alteration of the secondary structure and packing of the catalytic core. Mol. Cell *6*, 139–148.
17. Serre, L., Vellieux, F.M.D., Medina, M., Gomez-Moreno, C., Fontecilla-Camps, J.C., and Frey, M. (1996). X-ray structure of the Ferredoxin:$NADP^+$ Reductase from the cyanobacterium *anabaena* PCC 7119 at 1.8 Å resolution, and crystallographic studies of $NADP^+$ binding at 2.25 Å resolution. J. Mol. Biol. *263*, 20–39.
18. Hon, W.-C., McKay, G.A., Thompson, P.R., Sweet, R.M., Yang, D.S.C., Wright, G.D., and Berghuis, A.M. (1997). Structure of an enzyme required for aminoglycoside antibiotic resistance reveals homology to eukaryotic protein kinases. Cell *89*, 887–895.
19. Lu, F., Schumacher, M.A., Arvidson, D.N., Haldimann, A., Wanner, B.L., Zalkin, H., and Brennan, R.G. (1998). Structure-based redesign of corepressor specificity of the escherichia coli purine repressor by substitution of residue 190. Biochemistry *37*, 971–982.
20. Subramanya, H.S., Doherty, A.J., Ashford, S.R., and Wigley, D.B. (1996). Crystal structure of an ATP-dependent DNA ligase from bacteriophage T7. Cell *85*, 607–615.
21. Arni, R., Heinemann, U., Tokuota, R., and Saenger, W. (1988). Three-dimensional structure of the ribonuclease T_1-2′-GMP complex at 1.9-Å resolution. J. Biol. Chem. *263*, 15358–15368.
22. Huang, Q., Liu, S., Tang, Y., Jin, S., and Wang, Y. (1995). Studies on crystal structures, active-centre geometry and depurinating mechanism of two ribosome-inactivating proteins. Biochem. J. *309*, 285–298.
23. Hu, G., Oguro, A., Li, C., Gershon, P.D., and Quiocho, F.A. (2002). The "cap-binding slot" of an mRNA cap-binding protein: quantitative effects of aromatic side chain choice in the double-stacking sandwich with cap. Biochemistry *41*, 7677–7678.
24. Chakrabarti, P., and Uttamkumar, S. (1995). CH/π interaction in the packing of the adenine ring in protein structures. J. Mol. Biol. *251*, 9–14.
25. Burk, D.L., Hon, W.C., Leung, A.K.-W., and Berghuis, A.M. (2001). Structural analyses of nucleotide binding to an aminoglycoside phosphotransferase. Biochemistry *40*, 8756–8764.
26. McKay, G.A., Thompson, P.R., and Wright, G.D. (1994). Broad spectrum aminoglycoside phosphotransferase type III from *enterococcus*: overexpression, purification, and substrate specificity. Biochemistry *33*, 6936–6944.
27. McKay, G.A., and Wright, G.D. (1996). Catalytic mechanism of enterococcal kanamycin kinase (APH(3′)-IIIa): viscosity, thio, and solvent isotope effects support a Theorell-Chance mechanism. Biochemistry *35*, 8680–8685.
28. Azucena, E., and Mobashery, S. (2001). Aminoglycoside-modifying enzymes: mechanisms of catalytic processes and inhibition. Drug Resist. Updat. *4*, 106–117.
29. Wright, G.D., Berghuis, A.M., and Mobashery, S. (1998). Aminoglycoside antibiotics: structures, functions and resistance. Adv. Exp. Med. Biol. *456*, 27–69.
30. Llano-Sotelo, B., Azucena, E., Kotra, L.P., Mobashery, S., and Chow, C.S. (2002). Aminoglycoside modified by resistance enzymes display diminished binding to the bacterial ribosomal aminoacyl-tRNA site. Chem. Biol. *9*, 455–463.
31. Wright, G.D. (2000). Resisting resistance: new chemical strategies for battling superbugs. Chem. Biol. *7*, R127–R132.
32. Daigle, D.M., McKay, G.A., Thompson, P.R., and Wright, G.D. (1999). Aminoglycoside antibiotic phosphotransferases are also serine protein kinases. Chem. Biol. *6*, 11–18.
33. Boehr, D.D., Thompson, P.R., and Wright, G.D. (2001). Molecular mechanism of aminoglycoside antibiotic kinase APH(3′)-IIIa: roles of conserved active site residues. J. Biol. Chem. *276*, 23929–23936.
34. Thompson, P.R., Boehr, D.D., Berghuis, A.M., and Wright, G.D. (2002). Mechanism of aminoglycoside antibiotic kinase APH(3′)-IIIa: role of the nucleotide positioning loop. Biochemistry *41*, 7001–7007.
35. Liu, M., Haddad, J., Azucena, E., Kotra, L.P., Kirzhner, M., and Mobashery, S. (2000). Tethered bisubstrate derivatives as probes for mechanism and as inhibitors of aminoglycoside 3′-phosphotransferases. J. Org. Chem. *65*, 7422–7431.
36. Roestamadji, J., Graspas, I., and Mobashery, S. (1995). Loss of individual electrostatic interactions between aminoglycoside antibiotics and resistance enzymes as an effective means to overcoming bacterial drug resistance. J. Am. Chem. Soc. *117*, 11060–11069.
37. Roestamadji, J., and Mobashery, S. (1998). The use of neamine as a molecular template: inactivation of bacterial antibiotic resistance enzyme aminoglycoside 3′-phosphotransferase type IIa. Bioorg. Med. Chem. Lett. *8*, 3483–3488.
38. Sucheck, S.J., Wong, A.L., Koeller, K.M., Boehr, D.D., Draker, K.-A., Sears, P., Wright, G.D., and Wong, C.-H. (2000). Design of bifunctional antibiotics that target bacterial rRNA and inhibit resistance-causing enzymes. J. Am. Chem. Soc. *122*, 5230–5231.
39. Boehr, D.D., Lane, W.S., and Wright, G.D. (2001). Active site labeling of the gentamicin resistance enzyme AAC(6′)-APH(2″) by the lipid kinase inhibitor wortmannin. Chem. Biol. *8*, 791–800.
40. Daigle, D.M., McKay, G.A., and Wright, G.D. (1997). Inhibition of aminoglycoside antibiotic resistance enzymes by protein kinase inhibitors. J. Biol. Chem. *272*, 24755–24758.
41. Pullman, B., and Pullman, A. (1969). Quantum-mechanical investigations of the electronic structure of nucleic acids and their constituents. Prog. Nucleic Acid Res. Mol. Biol. *9*, 327–403.
42. Mecozzi, S., West, A.P., and Dougherty, D.A. (1996). Cation-π interactions in aromatics of biological interest: electrostatic potential surfaces as a useful qualitative guide. Proc. Natl. Acad. Sci. USA *93*, 10566–10571.
43. Rose, I.A., Hanson, K.R., Wilkinson, K.D., and Wimmer, M.J. (1980). A suggestion for naming faces of ring compounds. Proc. Natl. Acad. Sci. USA *77*, 2439–2441.
44. McKay, G.A., and Wright, G.D. (1995). Kinetic mechanism of aminoglycoside phosphotransferase type IIIa: evidence for a Theorell-Chance mechanism. J. Biol. Chem. *270*, 24686–24692.
45. Dill, K.A. (1990). Dominant forces in protein folding. Biochemistry *29*, 7133–7155.
46. Shaw, K.J., Rather, P.N., Hare, R.S., and Miller, G.H. (1993). Molecular genetics of aminoglycoside resistance genes and familial relationships of the aminoglycoside-modifying enzymes. Microbiol. Rev. *57*, 138–163.
47. Blakaj, D.M., McConnell, K.J., Beveridge, D.L., and Baranger, A.M. (2001). Molecular dynamics and thermodynamics of protein-RNA interactions: mutation of a conserved aromatic residue modifies stacking interactions and structural adaptation in the U1A-stem loop 2 RNA complex. J. Am. Chem. Soc. *123*, 2548–2551.
48. LeCuyer, K.A., Behlen, L.S., and Uhlenbeck, O.C. (1996). Mutagenesis of a stacking contact in the MS2 coat protein-RNA complex. EMBO J. *15*, 6847–6853.
49. Burkard, M.E., Kierzek, R., and Turner, D.H. (1999). Thermodynamics of unpaired terminal nucleotides on short RNA helixes correlates with stacking at helix termini in larger RNAs. J. Mol. Biol. *290*, 967–982.
50. Friedman, R.A., and Honig, B. (1995). A free energy analysis of nucleic acid base stacking in aqueous solution. Biophys. J. *69*, 1528–1535.
51. Chipot, C., Jaffe, R., Maigret, B., Pearlman, D.A., and Kollman, P.A. (1996). Benzene dimer: a good model for π-π interactions in proteins? A comparison between the benzene and the toluene dimers in the gas phase and in an aqueous solution. J. Am. Chem. Soc. *118*, 11217–11224.

52. Tsuzuki, S., Honda, K., Uchimaru, T., Mikami, M., and Tanabe, K. (2002). Origin of the attraction and directionality of the π/π interaction: model chemistry calculations of benzene dimer interaction. J. Am. Chem. Soc. *124*, 104–112.
53. Hunter, C.A., and Sanders, J.K.M. (1990). The nature of π-π interactions. J. Am. Chem. Soc. *112*, 5525–5534.
54. Newcomb, L.F., and Gellman, S.H. (1994). Aromatic stacking interactions in aqueous solution: evidence that neither classical hydrophobic effects nor dispersion forces are important. J. Am. Chem. Soc. *116*, 4993–4994.
55. Gellman, S.H., Haque, T.S., and Newcomb, L.F. (1996). New evidence that the hydrophobic effect and dispersion are not major driving forces for nucleotide base stacking. Biophys. J. *71*, 3523–3526.
56. McKay, S.L., Haptonstall, B., and Gellman, S.H. (2001). Beyond the hydrophobic effect: attractions involving heteroaromatic rings in aqueous solution. J. Am. Chem. Soc. *123*, 1244–1245.
57. Price, S.L., and Stone, A.J. (1987). The electrostatic interactions in van der Waals complexes involving aromatic molecules. J. Chem. Phys. *86*, 2859–2868.
58. Hobza, P., and Sponer, J. (1999). Structure, energetics and dynamics of the nucleic acid base bairs: nonempirical ab initio calculations. Chem. Rev. *99*, 3247–3276.
59. Cozzi, F., Cinquini, M., Annunziata, R., Dwyer, T., and Siegel, J.S. (1992). Polar/π interactions between stacked aryls in 1,8-diarylnaphthalenes. J. Am. Chem. Soc. *114*, 5729–5733.
60. Pang, Y.-P., Miller, J.L., and Kollman, P.A. (1999). Computational and experimental studies of (2,2)-bis(indol-1-yl-methyl)acetate suggest the importance of the hydrophobic effect in aromatic stacking interactions. J. Am. Chem. Soc. *121*, 1717–1725.
61. Martin, C.B., Mulla, H.R., Willis, P.G., and Cammers-Goodwin, A. (1999). Derivatives of n-benzyl-2-phenylpyridinium bromide, minimalist models for face-to-face, center-to-edge π stacking in water. J. Org. Chem. *64*, 7802–7806.
62. Hunter, C.A., Lawson, K.R., Perkins, J., and Urch, C.J. (2001). Aromatic interactions. J. Chem. Soc., Perkin Trans. I *2*, 651–669.
63. Breault, G.A., Hunter, C.A., and Mayers, P.C. (1998). Influence of solvent on aromatic interactions in metal tris-bipyridine complexes. J. Am. Chem. Soc. *120*, 3402–3410.
64. Rashkin, M., and Waters, M.L. (2002). Unexpected substituent effects in offset π-π stacked interactions in water. J. Am. Chem. Soc. *124*, 1860–1861.
65. Kim, E., Paliwal, S., and Wilcox, C.S. (1998). Measurements of molecular electrostatic field effects in edge-to-face aromatic interactions and CH-π interactions with implications for protein folding and molecular recognition. J. Am. Chem. Soc. *120*, 11192–11193.
66. Ferguson, S.B., and Diederich, F. (1986). Electron donor-acceptor interactions in host-guest complexes in organic solvents. Angew. Chem. Int. Ed. *25*, 1127-1129.
67. Chelli, R., Gervasio, F.L., Procacci, P., and Schettino, V. (2002). Stacking and T-shape competition in aromatic-aromatic amino acid interactions. J. Am. Chem. Soc. *124*, 6133–6134.
68. Berman, H.M., Westbrook, J., Feng, Z., Gilliland, G., Bhat, T.N., Weissig, H., Shindyalov, I.N., and Bourne, P.E. (2000). The Protein Data Bank. Nucleic Acids Res. *28*, 235–242.
69. Hendlich, M. (1998). Databases for protein-ligand complexes. Acta Crystallogr. D Biol. Crystallogr. *54*, 1178–1182.
70. Martz, E. (2002). Protein explorer: easy yet powerful macromolecular visualization. Trends Biochem. Sci. *27*, 107–109.
71. Wiseman, T., Williston, S., Brandts, J., and Lin, L.-N. (1989). Rapid measurement of binding constants and heats of binding using a new titration calorimeter. Anal. Biochem. *179*, 131–137.
72. Creighton, T.E. (1993). Proteins: Structures and Molecular Properties, Second Edition. (New York: W.H. Freeman and Company).